water

MDPI

Article

Modelling Flood-Induced Wetland Connectivity and Impacts of Climate Change and Dam

Fazlul Karim [1,*], Steve Marvanek [2], Linda E. Merrin [1], Daryl Nielsen [3], Justin Hughes [1], Danial Stratford [1] and Carmel Pollino [1]

1 CSIRO Land and Water, Commonwealth Scientific and Industrial Research Organisation, Canberra, ACT 2601, Australia; Linda.Merrin@csiro.au (L.E.M.); Justin.Hughes@csiro.au (J.H.); Danial.Stratford@csiro.au (D.S.); Carmel.Pollino@csiro.au (C.P.)
2 CSIRO Land and Water, Commonwealth Scientific and Industrial Research Organisation, Glen Osmond, SA 5064, Australia; Steve.Marvanek@csiro.au
3 CSIRO Land and Water, Commonwealth Scientific and Industrial Research Organisation, Albury, NSW 2640, Australia; dnielsen1958@gmail.com
* Correspondence: Fazlul.Karim@csiro.au; Tel.: +61-2-6246-4526

Received: 26 March 2020; Accepted: 28 April 2020; Published: 30 April 2020

Abstract: Hydrological connectivity between rivers and wetlands is considered one of the key critical factors for the integrity of floodplain landscapes. This study is a comprehensive modelling exercise on quantifying flood-induced wetland connectivity and the potential impacts of climate and water storage in an unregulated river basin in northern Australia. Flood inundation was simulated using a two-dimensional hydrodynamic model and the connectivities between wetlands and rivers were calculated using geoprocessing tools in ArcGIS. Wetlands in the floodplain were identified using waterbody maps derived from satellite imagery. A broadly representative sample of 20 wetlands were selected from 158 wetlands in the Mitchell basin considering location, size and spatial distribution. Five flood events ranging from 1 in 2 to 1 in 100 years were investigated to evaluate how connectivity changes with flood magnitude. Connectivities were assessed for the current condition as well as for two scenarios of future climate (Cwet and Cdry) and one scenario of dam storage. Results showed that a 1 in 100 years event inundated about 5450 km^2 of land compared to 1160 km^2 for a 1 in 2 years event. Average connectivity of wetlands in the Mitchell basin varies from 1 to 5 days for the floods of 1 in 2 to 1 in 26 years. As expected, a large flood produces longer duration of connectivity relative to a small flood. Results also showed that reduction in mean connectivity under a dryer climate (up to 1.8 days) is higher than the possibility of increase under a wet climate (up to 1 day). The impacts of a water storage, in the headwater catchment, are highly pronounced in terms of inundation and wetland connectivity (e.g., mean connectivity reduced by 1.7 days). The relative change in connectivity is higher for a small flood compared to that of a large event. These results demonstrate that there is a possibility of both increase and decease in connectivity under future climate. However, any water storage will negatively impact the connectivity between floodplain waterbodies and thus reduce the material exchange resulting in a reduction in primary and secondary productions in rivers and wetlands.

Keywords: climate change; connectivity; flood; hydrodynamic modelling; wetland

1. Introduction

Floodplain wetlands provide an essential habitat for a range of aquatic and terrestrial biota and facilitate nutrients between waterbodies [1,2]. They provide essential physical and biological links between rivers and off-stream wetlands that facilitate the abundance and biodiversity of

many aquatic species [3,4]. In addition to promoting high biodiversity [5,6], floodplain wetlands also contribute to improving water quality by filtering sediments and nutrient sequestration [7,8]. However, with increased land demand for agricultural production, wetland habitats are decreasing all over the world [9–11]. Globally, there is a continuous trend of increasing land usage for infrastructure development and industrial expansion. Wetland habitats are also threatened due to increasing demand for floodplain land for agricultural production [12]. It is anticipated that climate change will alter the flow regimes across the landscape and there a is possibility of declining connectivity [13–16].

Flood-induced connectivity between wetlands and rivers has been identified as being a crucial element of river-floodplain ecosystem. Habitat heterogeneity in many wetlands across the world is produced by the changing water sources and connecting flow paths between waterbodies [17,18]. Natural connectivity between waterbodies are invariably important for aquatic species and any reduction in connectivity causes a decrease in biodiversity [19,20]. Several studies [21–23] reported that a high level of connectivity facilitates fish movement between water bodies to take refuge from predators. High-level connectivity is also important for fish spawning and growth. The information on how well (e.g., duration, timing) a wetland is connected to a river and how the connectivity varies with changes in streamflow is important to maintain the habitat quality and bioecological functioning of floodplain wetlands. This information is not available for a majority of floodplain wetlands across the world because of high cost and difficulties in monitoring a large number of wetlands. Moreover, it is estimated that catchment runoff could be decreased by up to 35% and this change may have serious implications on frequency and duration of inundation and wetland connectivity [24–26].

With recent developments in remote-sensing technologies, satellite imagery is widely used to acquire information on flood inundation [27,28]. However, freely available imagery is still not suitable for quantifying wetland connectivity. One key limitation of satellite imagery is that it is not dynamic and only suitable for estimating inundation when flow is not changing rapidly. In addition, coarse spatial resolution is an issue for quantifying channelized connectivity. Some satellite imageries are also affected by cloud cover. Therefore, it is not suitable for these remotely sensed methods to quantify the timing and duration of connectivity. Some studies [29,30] used hydrological modelling and Geographic Information System (GIS)-based analysis to quantify how inundation and waterbody connectivity change with streamflow. Shaikh et al. [31] used a similar approach to quantify the number of wetlands connected to a river at a variable flow rate. However, these models are not spatially explicit and estimate the inundation by relating stage height with a terrain model which is not suitable for regulated catchments or if there is irregular variation in land topography. It is important to note that the accuracy of spatial inundation modelling largely depends on the resolution of topographic data [32,33]. Recent advancement in computing facilities and the availability of high-resolution topography data provide the opportunities to estimate flood inundation and wetland connectivity with high spatial and temporal resolution using hydrodynamic modelling tools [34–36]. Recently, Karim et al. [37] used these opportunities and developed a method to quantify flood-induced wetland connectivity using a two-dimensional hydrodynamic model. However, their study is based on regular grid modelling which is not suitable to reproduce small wetlands and floodplain creeks in the model. The use of a flexible mesh (i.e., irregular grids) model can overcome many of the limitations of regular grid models as they allow the computational mesh to be aligned and refined to suit the geometry of the floodplain [38,39].

In this study, advanced inundation modelling techniques (e.g., flexible mesh model) were used to improve the accuracy of inundation dynamics. The study evaluated wetland connectivity in the Mitchell river basin in Queensland and estimated potential changes in connectivity due to climate change and artificial water storage in the headwater catchment. Moreover, their study has not investigated the role of secondary flood peaks on connectivity which is significantly increase the duration of connectivity. This manuscript is structured as follows: Section 2 describes physical and hydrological characteristics of the study area. The methods are described in Section 3 followed by the results in Section 4. Key findings are discussed in Section 5. The manuscript ends with a set of conclusions in Section 6.

2. Study Area

This study focused on the Mitchell river basin in tropical Australia. It encompasses an area of 71,530 km^2 and extends from Mareeba in the headwater catchment to Kowanyama at the outlet to the Gulf of Carpentaria (Figure 1). Major tributaries of the Mitchell River are the Palmer and Lynd rivers with contributing areas of 45,145 km^2. About 95% of the catchment land is occupied by pastures and shrubs. About 3% of the land is conservation reserve. This area is characterised by two distinctive seasons, wet and dry. The average rainfall in the catchment varies in the range of 1000 mm per year and about 90% of total rainfall occurs during the wet season (November to April). Annual potential evaporation is about 1750 mm with a strong seasonal pattern, ranging from monthly average of 200 mm during October to December to about 100 mm during the dry season [40].

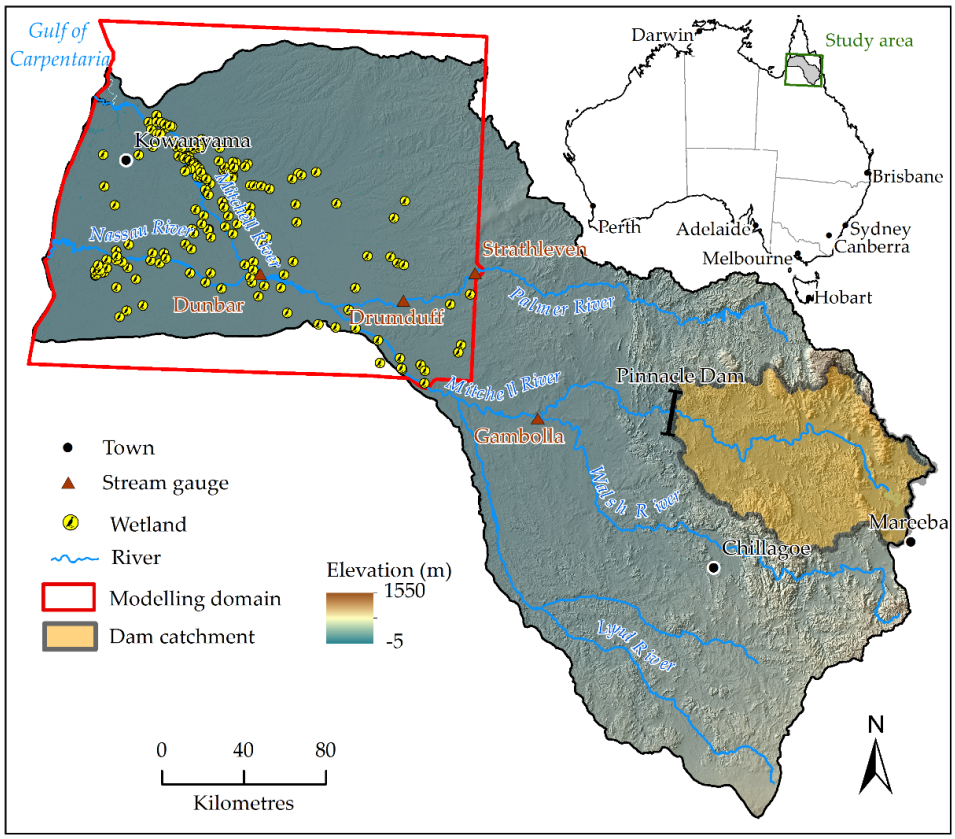

Figure 1. Mitchell river basin showing major rivers, stream gauges, floodplain wetlands and the boundary of the modelling.

The Mitchell River is perennial at its downstream reaches below the Dunbar. The mean annual flow at Dunbar is 7.11 km^3 with a maximum flow rate of 6387 m^3/s. The Mitchell River and its tributaries produce high flow annually during the wet season and cause widespread flooding at places across the catchments and at the floodplains of the Mitchell and Nassau river (a distributary of the Mitchell River). A total of 21 floods (ranging from small to large) were recorded in parts of the Mitchell river basin between 1981 and 2015 including large floods in 1999, 2000, 2009 and 2011. Observed flow record indicates intense and frequent floods since 1999 (Figure 2a). While floods can occur any time between November and April, about 89% of historical floods have occurred between January and March (Figure 2b). It takes approximately two and half days for the flood peak to travel from Dunbar to Kowanyama with an average speed of 1.7 km/hour.

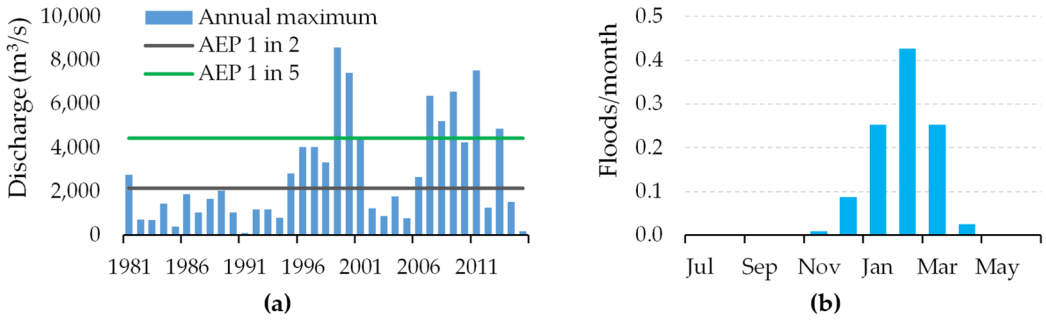

Figure 2. Historical floods in the Mitchell basin, (**a**) annual maximum discharge and (**b**) seasonal variation in flood frequency (AEP stands for annual exceedance probability).

Ecologically, the basin is characterized by tropical rainforest in the headwater catchments and open savanna in the Mitchell plains [41]. The floodplains of the Mitchell and Nassau rivers support large number of ecologically diverse habitats including off-stream wetlands that are connected to rivers either from overbank flow or channelized flow through creeks and floodplain pathways [42]. These wetlands provide an important source of primary production, nutrients and carbon which fuel aquatic food [43]. Wetlands in the Mitchell river basin are also important for economic and cultural value. The mangroves and coastal lagoons are also invaluable habitats to many terrestrial and aquatic biota.

3. Methods

The study was conducted using a floodplain hydrodynamic model combined with GIS-based analysis. Figure 3 illustrates the methods, showing three major components from model configuration to impact assessment. The first step is the configuring, calibrating and validating the model with several sets of input data followed by analysing the wetland connectivity. The third component of the study was scenario modelling for different climate and construction of a water storage on the Mitchell River.

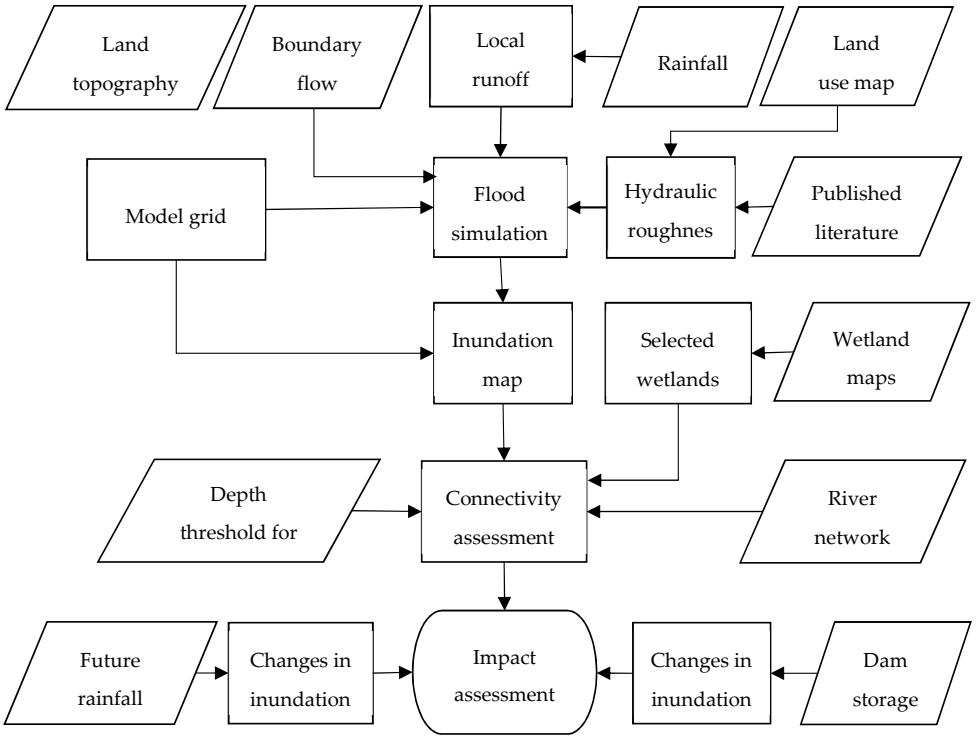

Figure 3. Flowchart illustrating the method of quantifying hydrological connectivity and impact assessment for future climate and water storage scenarios.

3.1. Input Data

One of the key inputs to any hydrodynamic model is the grid-based land topography. In this study, 30 m grid SRTM (Shuttle Radar Topography Mission) and 1 m grid LiDAR (Light Detection And Ranging) data [44] were used. A 5 m resolution digital elevation model (DEM) was produced by combining the SRTM and LiDAR DEMs to represent land surface elevation in the model. Due to the high cost of acquiring LiDAR data, it was collected only for the rivers and floodplains near the main river channels and was augmented with the coarser-scale SRTM DEM covering the remaining hydrodynamic model domain. The area covered by LiDAR is 600 km^2, which is about 16% of the model domain. Detail of the topography data processing can be found in Karim et al. [45]). Another important input to the model is the hydraulic roughness of the land surface. The roughness coefficients were derived from a remotely sensed land-use map [46] and were represented in the model using Manning's coefficient (n). Based on the land-use map, each grid cell in the model was categorised as one of the following land-cover categories: river, creek, wetlands, riparian vegetation, agriculture, bare soil and savanna. Initial roughness coefficients were estimated based on published literature ([47,48] and then refined as a part of the calibration process. Local runoff in the modelling domain was estimated using daily rainfall data and inflow boundaries were specified using observed daily streamflow data. Downstream boundaries were specified using hourly tide data.

3.2. Inundation Modelling

3.2.1. Model Configuration and Simulation

Flood inundation was simulated using a two-dimensional hydrodynamic model (MIKE21 FM) [49]. The model was configured for the downstream reaches of the Mitchell, Palmer and Nassau rivers covering an area of 32,000 km^2 (~0.9 million triangular mesh with elements of 72 m^2 for the smallest mesh and 1.3 km^2 for the largest mesh) which is about 44% of the Mitchell basin. Water depths for the entire modelling domain were simulated at a five-second time step by satisfying numerical stability criteria for the biggest flood in the analysis. Each event was simulated for 40 days (longer than the flooding period) irrespective of the time of flood recession time to ensure the entire rising and falling limbs were simulated. The first 5 days of simulation were considered as a warm-up period and, therefore, data over the first 5 days were not used in subsequent analysis. The models were run using a graphics processing unit GPU machine and, it took about 2 to 3 days of computer time for a simulation of 40 days. The model produced water depth information at the vertices of the triangular mesh. These results were further processed in ArcGIS to produce grid based (30 × 30 m) inundation depth.

Observed stage heights and inundation maps derived from the Moderate Resolution Imaging Spectroradiometer (MODIS) and Landsat imagery were used to calibrate the hydrodynamic model. In the calibration process, model grids that represent rivers and creeks were edited manually to remove any artefact during model mesh preparation. This ensures a continuous flow path in the model which is essential for maintaining the river conveyance. Final calibration was done by twigging the surface roughness coefficient (Manning's number). Detail of model calibration methods and results are presented in Karim et al. [45] and connectivity results are presented in this paper.

3.2.2. Floods Events of Scenario Modelling

During the wet season, flows occur overbank at places along the Mitchell, Palmer and Nassau rivers and inundate a large area of the floodplain downstream of Dunbar. Historical floods in the past 115 years (1901–2015) were identified by analyzing historical flow data at Dunbar on the Mitchell River. Recurrence interval of individual floods was estimated using the magnitude to frequency relationship. Flood data were examined within a magnitude–frequency framework which requires the estimate of the average recurrence interval for each flood. The recurrence interval (T_r) of a flood is defined as the average time interval which the flood of same magnitude or higher occurs at least once in that time

period. Based on a flood data series of descending order, the recurrence interval is calculated using a plotting position formula presented in Equation (1) [50].

$$T_r = \frac{n + 12}{m - 0.44} \quad (1)$$

where m is the rank of flood in the data series and n is the data length in year. A flood with a recurrence interval of T_r years was presented by Q_T. These flood data were fitted to a Pearson Type III (LP3) distribution to estimate the exceedance probability of an individual flood. To evaluate the significance of flood magnitude on wetland connectivity, six flood events of annual exceedance probability (AEP) of 0.5 (1 in 2), 0.2 (1 in 5), 0.1 (1 in 10), 0.05 (1 in 20), 0.02 (1 in 50) and 0.01 (1 in 100) were investigated. Time series of flood hydrographs were constructed based on a 2011 flood by scale-down and scale-up the maximum discharge of the 2011 flood to match the flood magnitude obtained from flood frequency distribution. It is important to note that the duration of connectivity largely differs between flood events of similar magnitude but a different number of secondary peaks [51]. To investigate this aspect, flood events of single peak, double peak and triple peaks were used (Figure 4).

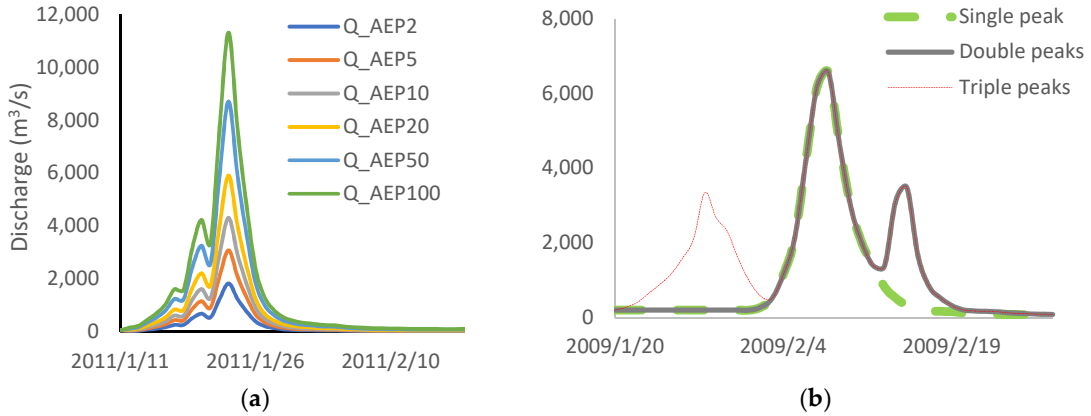

Figure 4. Inflow hydrographs for: (**a**) flood magnitude and (**b**) different number of peaks for the stream gauge at Gamboola on the Mitchell River.

3.3. Mapping Floodplain Wetland

Wetlands in the floodplain were identified using the Water Observations from Space (WOfS) product of Geoscience Australia which provides water-persistent depressions in the Australian landscape. The WOfS is a web service displaying historical surface water observations derived from Landsat 5 and Landsat 7 satellite imagery since 1987 [52]. A depression was considered as wetland if it retained water for a period of 50 days or more. Wetlands that appeared within the hydrodynamic modelling domain were selected for connectivity analysis (Figure 1). A primary list of wetlands was reproduced by cross checking with Google Earth imagery and topographic map. Based on a preliminary assessment of wetland persistence, 158 wetlands were initially selected for connectivity assessment. As there are large number of wetlands on the floodplains, connectivity results of 158 wetlands were assessed and a sub-set of 20 wetlands were selected for detailed analyses. Wetlands were selected to include a broadly representative sample that considered location within the floodplain, size and spatial distribution along the rivers (Table 1). The sample specifically included those wetlands close to the river channel through to wetlands on the outer floodplain. Selected wetlands were located along the Mitchell and Nassau rivers with a distance ranging from 0.8 km to 13.6 km from these two rivers.

Table 1. Wetlands in the Mitchell river basin and their geographical location on the floodplain.

Wetland ID	Longitude (°)	Latitude (°)	Nearest River	Area ($m^2 \times 10^4$)	Lateral Distance (km)
1	142.51	−15.96	Mitchell river	8.47	3.48
2	142.34	−15.90	Mitchell river	1.18	2.16
3	142.47	−15.95	Mitchell river	15.33	13.6
4	142.22	−15.70	Mitchell river	3.47	4.51
5	142.19	−15.64	Mitchell river	6.74	7.67
6	142.12	−15.60	Mitchell river	4.28	2.01
7	142.10	−15.54	Mitchell river	0.30	3.26
8	142.06	−15.48	Mitchell river	0.82	4.08
9	142.01	−15.46	Mitchell river	0.54	0.83
10	142.07	−15.41	Mitchell river	0.01	9.95
11	141.98	−15.41	Mitchell river	1.86	1.68
12	141.87	−15.40	Mitchell river	5.88	8.47
13	141.90	−15.35	Mitchell river	1.44	4.46
14	141.88	−15.27	Mitchell river	6.57	1.91
15	142.06	−15.96	Nassau river	7.25	1.88
16	141.93	−15.87	Nassau river	5.92	3.54
17	141.77	−15.84	Nassau river	1.50	6.66
18	141.74	−15.92	Nassau river	4.65	2.04
19	141.71	−15.87	Nassau river	2.93	2.61
20	141.62	−15.96	Nassau river	5.84	9.89

3.4. Connectivity Assessment

A wetland was considered connected to a river when a continuous flow path existed between the wetland and river. To identify connected waterbodies (e.g., wetlands, rivers) at each time step, an algorithm was developed in the ArcGIS environment to check contiguous grids in the entire modelling domain. For this purpose, a threshold water depth was used to distinguish connected water bodies from the rest the domain. Following consideration of the low resolution of the floodplain topographic data and the high roughness of the floodplain landscape due to vegetation cover, a threshold water depth of 10 cm was used in this study [53]. Figure 5 shows a schematic representation of identifying connection and disconnection of a wetland based on water depth. A wetland is considered connected to surrounding water bodies when it starts receiving flood water and considered disconnected when water depth falls below bank level. The wetland could be reconnected if there is any secondary flood peak (Figure 5).

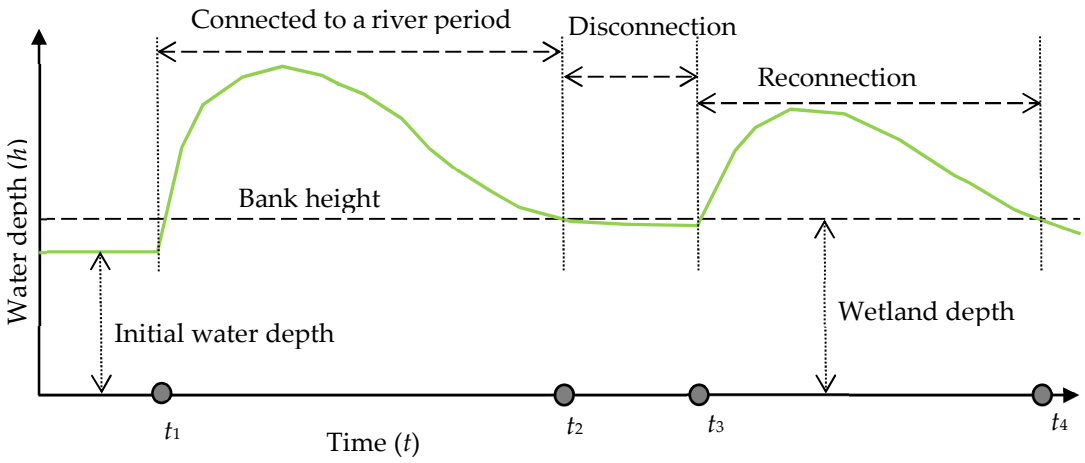

Figure 5. Flowchart illustrating the method of quantifying hydrological connectivity and impact assessment for future climate and water storage scenarios.

Connectivity was analysed using geoprocessing tools in ArcGIS. At each time step, computational grids were classified as either wet or dry based on water depth information generated from hydrodynamic modelling results. The 'pathdistance' function in the spatial analyst tool was used to calculate the nearest distance from a wetland to the nearest river. This attribute was added to the point features representing wetlands. If a wetland is not connected to any river for a time step, a null value was added for that particular time step. By accumulating this information for the entire flooding period, a time series of connection and disconnection for individual wetland was obtained.

3.5. Scenario Modelling

A series of scenarios were devised to explore how flood inundation and wetland connectivity could change under future climate and infrastructure developments. However, due to long simulation time of the hydrodynamic model, two scenarios for climate (wet and dry) and one scenario for dam storage (Pinnacle dam) were investigated to enable generalised conclusions. For each scenario, three flood events representing small, medium and large floods (1 in 2, 10 and 26 AEPs) were investigated.

The impacts of future climate were investigated using results from 21 global climate models (GCMs) for the Representative Concentration Pathway (RCP) of business as usual (RCP8.5) presented in the fifth assessment report (AR5) of the Intergovernmental Panel on Climate Change [54]. Future climate projections for all GCMs were downloaded from the Coupled Model Intercomparison Project (CMIP5) website (http://cmip-pcmdi.llnl.gov/cmip5/). Future projections for 21 GCMs were ranked from lowest to highest based on averaged mean annual rainfall over the period of 1890 to 2015. Three scenarios representing dry, mid and wet future conditions corresponding to GCMs results of 10th (dry), 50th (mid) and 90th (wet) percentile were selected for scenario modelling. Seasonal scaling factors estimated for four seasons—December to February (DJF), March to May (MAM), June to August (JJA) and September to November (SON)—were used to generate the daily time series of future rainfall in the period of 2046 to 2075 (centred at 2060). Detail of future rainfall prediction can be found in the companion study by [40]. The mean annual flow in the period of 1890 to 2015 under 'mid' climate (50th percentile rainfall) was found to be similar to observed mean annual flow in the study area. Therefore, mid climate was considered as baseline and comparison of 'wet' (Cwet) and 'dry' (Cdry) climates were performed with respect to mid climate. Streamflow at the model boundaries were simulated using the Australian Water Resources Assessment (AWRA) hydrological model [55]. Figure 6 shows an example of inflow hydrographs for Cwet and Cdry compared to baseline condition.

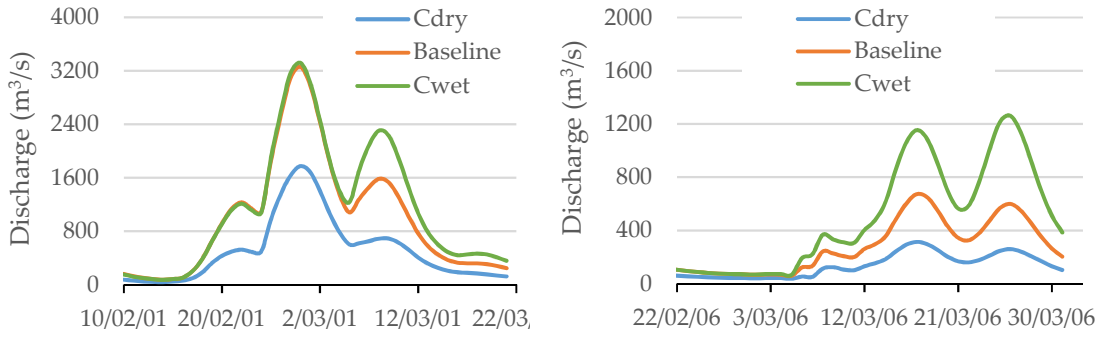

Figure 6. Typical flood hydrographs for climate scenario modelling for (**a**) 2001 (AEP of 1 in 10) and (**b**) 2006 (AEP of 1 in 2) events. Cdry and Cwet represent the changes in inflow to the floodplain with respect to baseline condition.

For this exploratory scenario a dam storage (reservoir) with a capacity of 2.32 km^3 was considered at the headwater catchment (Pinnacle dam, Figure 1) of the Mitchell River (approximately 130 km upstream of hydrodynamic model boundary). The reservoir was assumed to be half-full at the start

of each simulation. This is considered more realistic than simulating empty reservoirs (considered a more conservative approach) when assessing the impacts of dam operations during flood events. Only streamflow at the upstream boundaries of the hydrodynamic model domains were updated, whereas the remaining input datasets and boundary conditions in the calibrated hydrodynamic models remained unchanged. Three historical flood events (2006, 2001 and 2009) of different magnitudes (1 in 2, 10 and 26, respectively) were selected to assess in connectivity for different floods.

4. Results

4.1. Inundation Extent

Simulated water depth data from the hydrodynamic model results were accumulated for the entire flooding period (40 days) to estimate the maximum flooding extent for different floods. Figure 7 shows an example of floodplain inundation extent for five floods ranging from 1 in 2 to 1 in 100 AEPs. As expected, a big flood produces large inundation across the floodplain and creates more connectivity between off-stream wetlands and rivers. In this example, an event of 1 in 2 AEP inundated about 1160 km^2 of land and the inundated areas are 1806, 2412, 3067, 4308 and 5450 km^2 for an event of 1 in 5, 10, 20, 50, and 100 AEPs respectively. The Nassau River produced large areas of inundation along both banks. While a flood of any magnitude produces overbank inundation along the Mitchell River, significant inundation along the Nassau River were noticed only for large floods (e.g., AEP of 20 or more). Although selected wetlands were within the range of overbank inundation for a large flood (AEP of 20 or more), several wetlands were located outside the flooding extent of a regular flood (i.e., AEP of 2 or less). It is important to note that minor creeks could not be reproduced in the model due to coarse (30 m SRTM) topography data. Therefore, results presented here could be an underestimation of inundation area.

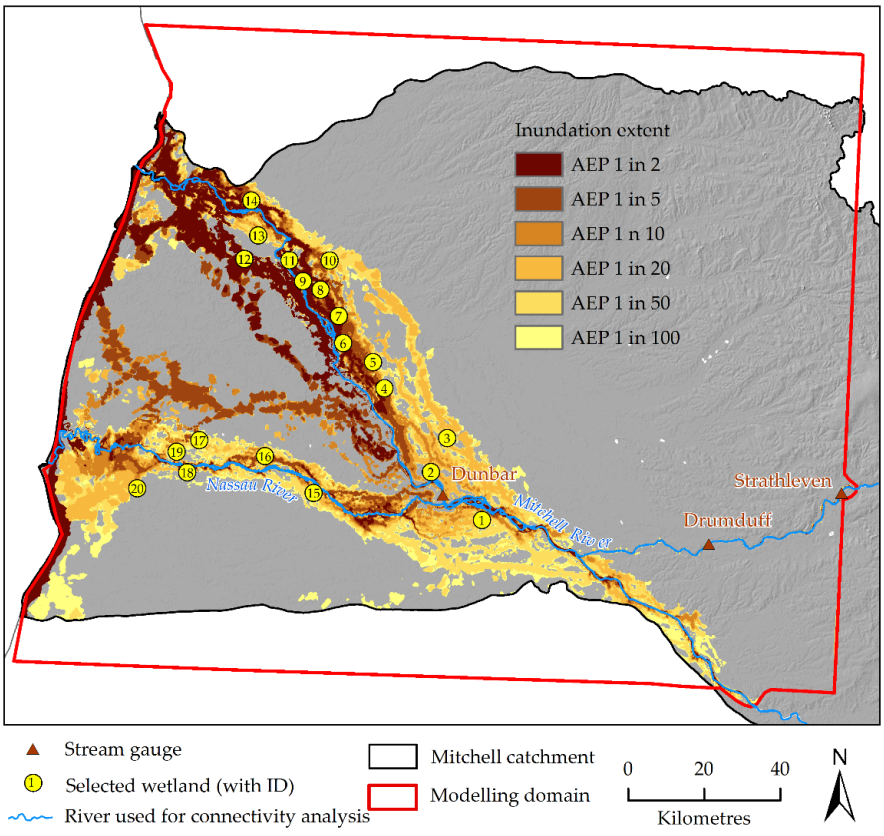

Figure 7. Inundation extent for the flooding events of different magnitude representing small, medium and large floods (AEP: annual exceedance probability).

4.2. Inundation Duration

Results show longer inundation duration for the floodplain along the lower reaches of the Mitchell and Nassau rivers (Figure 8). This behaviour is explained well by the flat topography in the downstream ends of the basin. While the Nassau River produced large inundation along the river banks, the duration of the inundation was relatively small compared to the Mitchell River. Like inundation extent, duration of inundation is longer for a large flood. However, duration of inundation is largely influenced by the secondary flood peaks. Figure 8 shows how inundation duration could be different for a flood of same magnitude but a different number of secondary peaks. Large proportions of the floodplain adjacent to the Mitchell river as well as between the Mitchell and Nassau rivers experienced flooding of more than 20 days for a flood of two secondary peaks (Figure 8b) while only a few pockets of low-lying land experienced similar inundation for the flood of a single peak (Figure 8a).

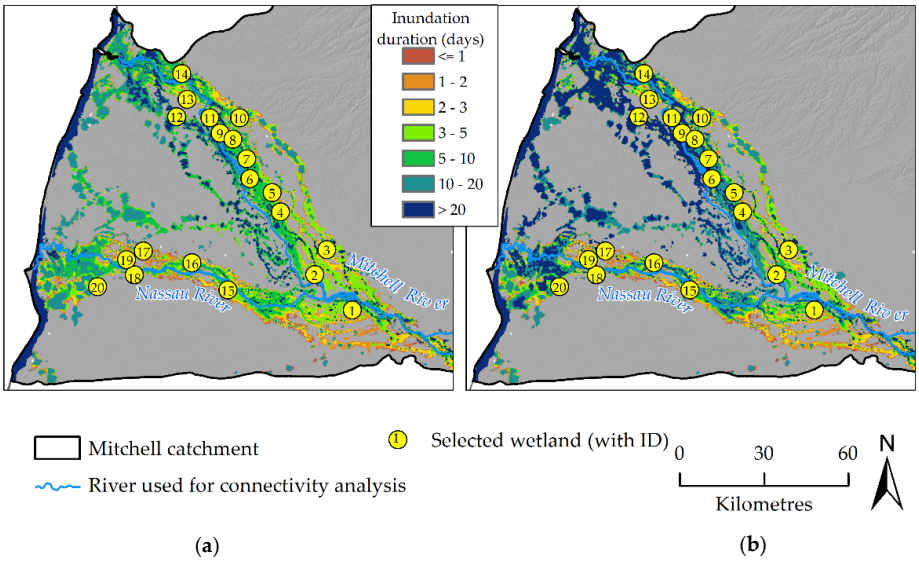

Figure 8. Inundation maps showing duration of flooding in the Mitchell basin for a flood event of (**a**) single peak and (**b**) multi peaks (refer to Figure 4 for flood hydrograph). Yellow circle shows the location of wetlands on the floodplain.

4.3. Wetland Connectivity

Figure 9 shows an example of connectivity analysis for the 20 selected wetlands based on inundation information for the flood event in 2009 (AEP 1 in 26). At each time step, connected and disconnected wetlands with rivers were identified and the information was accumulated to quantify the time sequence of connectivity of individual wetland. The left panel shows the connected and disconnected wetlands on 15 February 2009 (10 days since flood has started) and the right panel shows the same for 1 March 2019 (24 days since the flood has started). On the 10th day of the flood (rising flood), 9 wetlands were connected to the Mitchell and Nassau rivers and on 24th day (receding flood), 12 wetlands were connected to the river. It is important to note that some wetlands could be inundated by flood water but designated as not connected (e.g., 48 on the left panel). This is because the inundation is not continuous between the wetland and the river.

Figure 10 shows a summary of wetland connectivity in the Mitchell basin for different floods. The flood event of 2006 (AEP of 1 in 2) produced the least connectivity and the 2009 flood (AEP of 1 in 26) produced the highest connectivity. As seen previously, large floods inundate more area, and they also create longer duration of connectivity. Wetlands that were not connected in the 2006 and 2001 floods were connected in the 2009 flood primarily due to the large flood magnitude. Several wetlands show disconnection and reconnection because of multiple peaks in flow hydrographs.

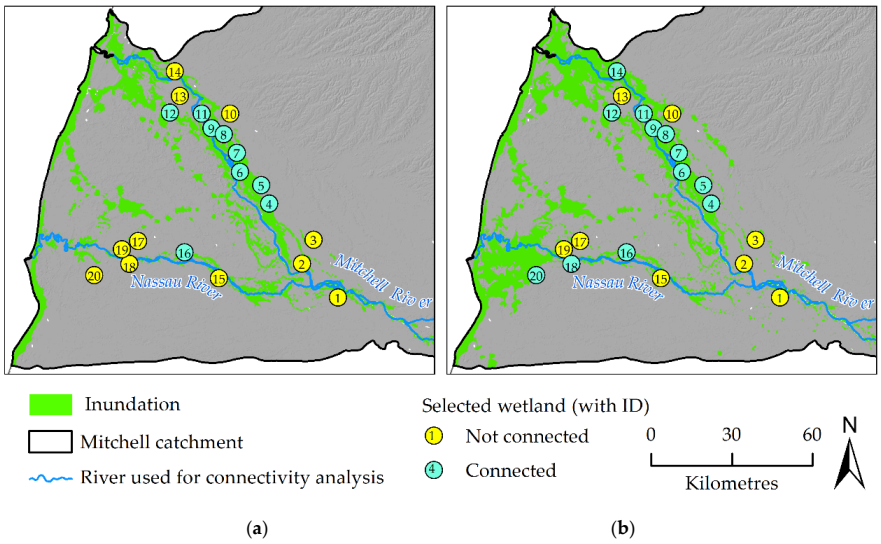

Figure 9. Method of connectivity analysis based on inundation information for the 2009 flood. Connected wetlands are shown for (**a**) 15 February 2009 and (**b**) 1 March 2009.

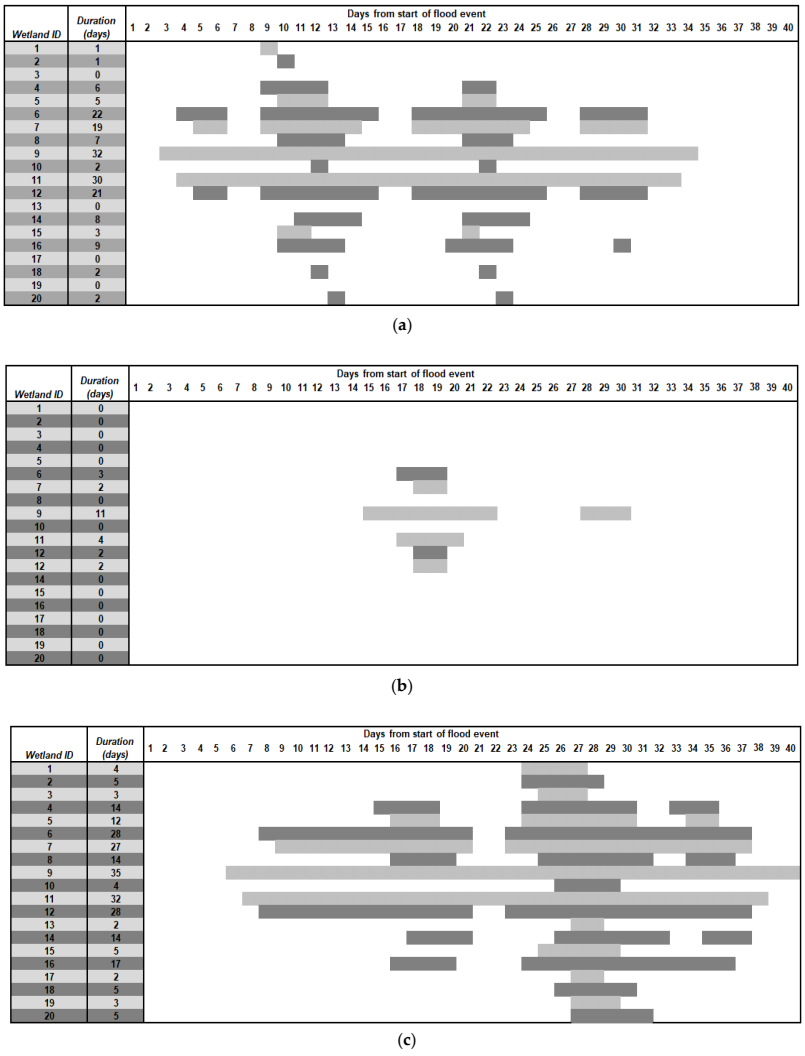

Figure 10. Timing and duration of connectivity of 20 selected wetlands in the Mitchell river basin for the (**a**) 2001 flood (AEP of 1 in 10), (**b**) 2006 flood (AEP of 1 in 2) and (**c**) 2009 flood (AEP of 1 in 26).

Results show that average connectivity of wetlands in the Mitchell basin varies from 1 to 5 days for the floods of 1 in 2 to 1 in 10 AEP. As expected, a large flood produces longer duration of connectivity relative to a small flood (Figure 2). Increases in flood size and estimated change due the future climate and dam construction are presented in Table 2 which presents a summary of predicted changes in connectivity for a wet climate (Cwet), dry climate (Cdry) and dam scenarios for the flood events of 1 in 2, 10 and 26 AEPs. As seen previously, a wet climate (Cwet) scenario increased the duration of inundation and consequently increased the connectivity. Similarly, a dry (Cdry) climate scenario reduced the connectivity. However, the impacts were more pronounced for a small flood (e.g., the 2006 event). A reduction in connectivity of approximately 50% was predicted for a dry climate (Table 2). The changes in connectivity vary between flood events and the magnitude of the flood varies. Results are consistent with the changes in flow regime as seen in Figure 6.

The impacts of the reservoir in the headwater catchment were found to be very high, a reduction of connectivity of up to 50% for a small flood event. In a wetter climate, dam impact could be offset to some extent. However, impacts are more pronounced for a combined scenario of dam and dry climate.

Table 2. Average connectivity of wetlands in the Mitchell basin and changes for climate and dam scenarios.

Flood Event	AEP (Years)	Mean Connectivity (Days)	Change in Connectivity, Days (%)				
			Cdry	Cwet	Dam	Cdry and Dam	Cwet and Dam
2001	1 in 10	3.2	−1.8 (56)	+0.5 (15)	−1.5 (47)	−2.2 (69)	−1.2 (39)
2006	1 in 2	1.2	−0.6 (53)	+1.0 (83)	−0.6 (51)	−0.9 (72)	+0.1 (11)
2009	1 in 26	4.9	−1.6 (33)	+0.03 (1)	−1.7 (34)	−2.7 (55)	−0.7 (15)

5. Discussion

This study provides useful information on inundation dynamics under altered flood regimes that will facilitate impact assessment on ecological assets (e.g., habitat quality, water quality, biodiversity). These kinds of information are especially important for the studies on estimating fish response and recruitment in off-stream floodplain wetlands as reported in [2,3]. Flood magnitude and the rate of rise of water level are the primary factors that influence the flooding extent in terms of inundation area and depth. While inundation area increases with increasing flood magnitude, the rate of increase depends on floodplain topography and artificial barriers (e.g., dikes, elevated roads, water storages etc.) as well as rate of rise of flood water. For example, magnitude of a 50-year flood (maximum discharge) which is 4.8 times larger compared to a 2-year flood in the Mitchell basin produced about 3.7 times inundation. This is because floodplain undulation and/or man-made barriers controls inundation as the water moves further away from the rivers. These results are consistent with other flood inundation studies for Australian river basins [34,37] and elsewhere [35]. However, results are different from that found by Karim et al. [51] for the Tully catchment in the Great Barrier Reef catchments. This is not surprising since the Tully catchment is relatively small and it has steep topography at the further end of the floodplain. Duration of inundation is mostly governed by the topography of the floodplain and to some extent the shape of the inflow hydrograph. Longer durations of inundation were found for the lands adjacent to the Mitchell River, primarily due to flat topography and low bank height of the river (up to 3 m lower compared to similar areas adjacent to the Nassau River).

Wetland connectivity results presented in this paper depend on threshold water depth that distinguish between connected and disconnected wetlands. The threshold (10 cm) was estimated considering fish movement between rivers and wetlands during overbank flooding. The threshold could be different based on the purpose of the study. For example, 1 or 2 cm depth could be sufficient for small fish, especially when channelized movement is considered [18,53]. In this study, a large threshold depth was used because of dense vegetation cover in a tropical floodplain. However, the choice of the threshold should be case specific.

The mean connectivity of the selected wetlands varied between 1.2 to 4.9 days based on flood magnitude (AEP of 1 in 2, 10 and 26). In general, wetlands that are located in the lower reaches of

the river experience longer duration of connectivity. This connectivity pattern is due to low-lying lands adjacent to the river. The Nassau River produced large areas of inundation on both sides of the river. However, the duration of inundation was relatively small compared to the Mitchell River. It is important to note that small floodplain creeks disappeared in the model due to the coarse topography data (30 m SRTM DEM). Therefore, some of wetlands that are identified as not connected with the river by overbank flow could be connected to the river through channelized flow.

The impacts of future climate and dam were highly pronounced across the floodplain. The impacts were more pronounced for a small flood (e.g., the 2006 event). A reduction in connectivity of approximately 50% was predicted under a dry climate. The changes in connectivity vary between flood events based on flood magnitude. The impacts of the dam were very high (up to 50%) compared to dams on other tropical river basins [45]. This is because the capacity of the dam in the Mitchell basin (2.32 km^3) is high. Infrastructure development, such as constructing a dam on a river can significantly reduce the flooding area and connectivity. While dam capacity is the major factor influencing the inundation dynamics, proportion of local runoff compared to inflows is another major factor that influences the connectivity.

6. Conclusions

In this study, an advanced flood inundation modelling technique is applied to quantify floodplain inundation and flood-induced wetland connectivity. The use of flexible mesh hydrodynamic modelling was found to be advantageous over a regular grid model to improve the accuracy of results. The study identified that fine-scale topographic data (e.g., LiDAR) is crucial for reproducing floodplain pathways (e.g., creek) in the model. Time sequences of connection and disconnection for individual wetlands were estimated by accumulating the information on contiguous waterbodies. The study evaluated connectivity of a large numbers of wetlands in the Mitchell basin and estimated potential changes in connectivity due to climate change and construction of a dam in the headwater catchment.

It has been confirmed that wetland connectivity to the main rivers is not only controlled by the flood magnitude but also floodplain characteristics and inflow from upstream catchments. Floodplain topography, rate of rise of flood water and secondary flood peaks are the key factors that influence the duration of flooding and wetland connectivity. Wetlands located in the downstream reaches of the floodplain showed a longer duration of connectivity primarily due to low-lying lands and additional water from local runoff. Another important factor is the flood pattern (e.g., rate of rise of water level, two or more flood peaks in a single event) that influence the connectivity significantly. Results indicate that a small change in rainfall could have large changes in inundation and wetland connectivity. Climate change could exacerbate the connectivity status for many off-stream wetlands, especially for wetlands that are currently least connected with a river. This information is useful for assessing recruitment patterns of aquatic biota and biodiversity of wetlands across the floodplain. It is expected that the information generated in this study will be taken by policy makers and natural resource management authorities to maintain an optimal connectivity level between rivers and offs-stream wetlands. While the study is case specific, the methods of quantifying connectivity and impact assessment can be used elsewhere.

Author Contributions: Conceptualization, F.K., C.P., D.N, and D.S.; methodology, F.K., J.H., S.M., L.E.M.; software, F.K., J.H. and L.M; validation, F.K. and S.M.; formal analysis, F.K., S.M. and J.H; investigation, F.K.; resources, F.K., D.N and L.M; data curation, F.K., S.M. and L.E.M.; writing—F.K.; writing—review and editing, F.K., S.M., C.P., D.N., D.S. and L.E.M.; visualization, F.K., S.M. and J.H; supervision, C.P.; project administration, F.K and J.H. All authors have read and agreed to the published version of the manuscript.

Funding: Research funding for this study was received from the Australian Government Department of Agriculture and Water Resources.

Acknowledgments: We thankfully acknowledge valuable input from Klaus Joehnk and Yingying Yu of CSIRO in an earlier version of this manuscript.

Conflicts of Interest: The authors declare no conflict of interest.

References

1. Waltham, N.J.; Burrows, D.; Wegscheidl, C.; Buelow, C.; Ronan, M.; Connolly, N.; Groves, P.; Marie-Audas, D.; Creighton, C.; Sheaves, M. Lost Floodplain Wetland Environments and Efforts to Restore Connectivity, Habitat, and Water Quality Settings on the Great Barrier Reef. *Front. Mar. Sci.* **2019**, *6*. [CrossRef]
2. Arthington, A.H.; Godfrey, P.C.; Pearson, R.G.; Karim, F.; Wallace, J. Biodiversity values of remnant freshwater floodplain lagoons in agricultural catchments: Evidence for fish of the Wet Tropics bioregion, northern Australia. *Aquat. Conserv. Mar. Freshw. Ecosyst.* **2014**, *25*, 336–352. [CrossRef]
3. Pearson, R.G.; Godfrey, P.C.; Arthington, A.H.; Wallace, J.; Karim, F.; Ellison, M. Biophysical status of remnant freshwater floodplain lagoons in the Great Barrier Reef catchment: A challenge for assessment and monitoring. *Mar. Freshw. Res.* **2013**, *64*, 208–222. [CrossRef]
4. Smardon, R. Wetland Ecology Principles and Conservation, Second Edition. *Water* **2014**, *6*, 813–817. [CrossRef]
5. Briggs, S.V.; Thornton, S.A. Management of water regimes in River Red Gum Eucalyptus camaldulensis wetlands for water bird breeding. *Aust. Zool.* **1999**, *31*, 187–197. [CrossRef]
6. Leigh, C.; Sheldon, F. Hydrological connectivity drives patterns of macroinvertebrate biodiversity in floodplain rivers of the Australian wet dry tropics. *Freshwater Biol.* **2009**, *54*, 549–571. [CrossRef]
7. Greenway, M.; Woolley, A. Constructed wetlands in Queensland: Performance efficiency and nutrient bioaccumulation. *Ecol. Eng.* **1998**, *12*, 19–55. [CrossRef]
8. McJannet, D.; Wallace, J.; Keen, R.; Hawdon, A.; Kemei, J. The filtering capacity of a tropical riverine wetland: II. Sediment and nutrient balances. *Hydrol. Process.* **2012**, *26*, 53–72. [CrossRef]
9. Bunn, S.E.; Arthington, A.H. Basic principles and ecological consequences of altered flow regimes for aquatic biodiversity. *Environ. Manag.* **2002**, *30*, 492–507. [CrossRef]
10. Opperman, J.J.; Galloway, G.E.; Fargione, J.; Mount, J.F.; Richter, B.D.; Secchi, S. Sustainable Floodplains Through Large-Scale Reconnection to Rivers. *Science* **2009**, *326*, 1487–1488. [CrossRef]
11. Tockner, K.; Lorang, M.S.; Stanford, J.A. River flood plains are model ecosystems to test general hydrogeomorphic and ecological concepts. *River Res. Appl.* **2010**, *26*, 76–86. [CrossRef]
12. Tockner, K.; Bunn, S.E.; Quinn, G.; Naiman, R.; Stanford, J.A.; Gordon, C. Floodplains: Critically threatened ecosystems. In *Aquatic Ecosystems*; Polunin, N.C., Ed.; Cambridge University Press: Cambridge, UK, 2008; pp. 45–61.
13. Burket, V.; Kusler, J. Climate change: Potential impacts and interactions in wetlands of the United States. *J. Am. Water Resour. Assoc.* **2000**, *36*, 313–320. [CrossRef]
14. Dawson, T.P.; Berry, P.M.; Kampa, E. Climate change impacts on freshwater wetland habitats. *J. Nat. Conserv.* **2003**, *11*, 25–30. [CrossRef]
15. Erwin, K.L. Wetlands and global climate change: The role of wetland restoration in a changing world. *Wetl. Ecol. Manag.* **2009**, *17*, 71–84. [CrossRef]
16. Kingsford, R.T. Conservation management of rivers and wetlands under climate change: A synthesis. *Mar. Freshw. Res.* **2011**, *62*, 217–222. [CrossRef]
17. Junk, W.J.; Bayley, P.B.; Sparks, R.E. The flood pulse concept in river-floodplain systems. *Can. Spec. Publ. Fish. Aquat. Sci.* **1989**, *106*, 110–127.
18. Lyon, J.; Stuart, I.; Ramsey, D.; O'Mahony, J. The effect of water level on lateral movements of fish between river and off-channel habitats and implications for management. *Mar. Freshwater Res.* **2010**, *61*, 271–278. [CrossRef]
19. Ward, J.V.; Tockner, K.; Schiemer, F. Biodiversity of floodplain river ecosystems: Ecotones and connectivity. *Regul. Rivers Res. Manag.* **1999**, *15*, 25–139. [CrossRef]
20. Pringle, C.M. Hydrologic connectivity and the management of biological reserves: A global perspective. Ecological Applications. *Ecol. Appl.* **2001**, *11*, 981–998. [CrossRef]
21. Balcombe, S.R.; Bunn, S.E.; Arthington, A.H.; Fawcett, J.H.; Mckenzie-Smith, F.J.; Wright, A. Fish larvae, growth and biomass relationships in an Australian arid zone river: Links between floodplains and waterholes. *Freshwater Biol.* **2007**, *52*, 2385–2398. [CrossRef]
22. Lasne, E.; Lek, S.; Laffaille, P. Patterns in fish assemblages in the Loire floodplain: The role of hydrological connectivity and implications for conservation. *Biol. Conserv.* **2007**, *139*, 258–268. [CrossRef]
23. Steffensen, K.D.; Eder, B.L.; Pegg, M.A. Fish community response to floodplain inundation in a regulated river. *J. Freshwater Ecol.* **2014**, *29*, 413–427. [CrossRef]

24. Van, P.D.T.; Popescu, I.; van Griensven, A.; Solomatine, D.P.; Trung, N.H.; Green, A. A study of the climate change impacts on fluvial flood propagation in the Vietnamese Mekong Delta. *Hydrol. Earth Syst. Sci.* **2012**, *16*, 4637–4649. [CrossRef]
25. Langerwisch, F.; Rost, S.; Gerten, D.; Poulter, B.; Rammig, A.; Cramer, W. Potential effects of climate change on inundation patterns in the Amazon Basin. *Hydrol. Earth Syst. Sci.* **2013**, *17*, 2247–2262. [CrossRef]
26. Rouillard, A.; Skrzypek, G.; Dogramaci, S.; Turney, C.; Grierson, P.F. Impacts of a changing climate on a century of extreme flood regime of northwest Australia. *Hydrol. Earth Syst. Sci. Discuss.* **2014**, *11*, 11905–11943. [CrossRef]
27. Schumann, G. Preface: Remote Sensing in Flood Monitoring and Management. *Remote Sens.* **2015**, *7*, 17013–17015. [CrossRef]
28. Bates, P.D. Remote sensing and flood inundation modelling. *Hydrol. Processes* **2004**, *18*, 2593–2597. [CrossRef]
29. Overton, I.C. Modelling floodplain inundation on a regulated river: Integrating GIS, remote sensing and hydrological models. *River Res. Appl.* **2005**, *21*, 991–1001. [CrossRef]
30. Frazier, P.; Page, K. A reach-scale remote sensing technique to relate wetland inundation to river flow. *River Res. Appl.* **2009**, *25*, 836–849. [CrossRef]
31. Shaikh, M.; Green, D.; Cross, H. A remote sensing approach to determine environmental flows for wetlands of the Lower Darling River, New South Wales, Australia. *Int. J. Remote Sens.* **2001**, *22*, 1737–1751. [CrossRef]
32. Van de Sande, B.; Lansen, J.; Hoyng, C. Sensitivity of Coastal Flood Risk Assessments to Digital Elevation Models. *Water* **2012**, *4*, 568–579. [CrossRef]
33. Teng, J.; Jakeman, A.J.; Vaze, J.; Croke, B.F.W.; Dutta, D.; Kim, S. Flood inundation modelling: A review of methods, recent advances and uncertainty analysis. *Environ. Modell. Softw.* **2017**, *90*, 201–216. [CrossRef]
34. Tuteja, N.K.; Shaikh, M. Hydraulic modelling of the spatiio-temporal flood inundation patterns of the Koondrook Perricoota forest wetlands- the living Murray. In *18th World IMACS, MODSIM Congress*; Modelling and Simulation Society of Australia and New Zealand: Cairns, Australia, 2009; pp. 4248–4254.
35. Hardesty, S.; Shen, X.; Nikolopoulos, E.; Anagnostou, E. A Numerical Framework for Evaluating Flood Inundation Hazard under Different Dam Operation Scenarios—A Case Study in Naugatuck River. *Water* **2018**, *10*, 1798. [CrossRef]
36. Mihu-Pintilie, A.; Cîmpianu, C.I.; Stoleriu, C.C.; Pérez, M.N.; Paveluc, L.E. Using High-Density LiDAR Data and 2D Streamflow Hydraulic Modeling to Improve Urban Flood Hazard Maps: A HEC-RAS Multi-Scenario Approach. *Water* **2019**, *11*, 1832. [CrossRef]
37. Karim, F.; Petheram, C.; Marvanek, S.; Ticehurst, C.; Wallace, J.; Hasan, M. Impact of climate change on floodplain inundation and hydrological connectivity between wetlands and rivers in a tropical river catchment. *Hydrol. Processes* **2016**, *30*, 1574–1593. [CrossRef]
38. Mackay, C.; Suter, S.; Albert, N.; Morton, S.K.Y. Large scale flexible mesh 2D modelling of the Lower Namoi Valley. In *Floodplain Management Association National Conference*; Floodplain Management Australia: Brisbane, Australia, 2015; pp. 1–14.
39. Symonds, A.M.; Vijverberg, T.; Post, S.; van der Spek, B.; Henrotte, J.; Sokolewicz, M. Comparison between Mike 21 FM, Delft3D and Delft3D FM flow models of Western Port Bay, Australia. In Proceedings of the 35th International Conference on Coastal Engineering, Antalya, Turkey, 17–20 November 2016; pp. 1–12.
40. Charles, S.; Petheram, C.; Berthet, A.; Browning, G.; Hodgson, G.; Wheeler, M.; Yang, A.; Gallant, S.; Marshall, A.; Hendon, H.; et al. *Climate Data and Their Characterisation for Hydrological and Agricultural Scenario Modelling across the Fitzroy, Darwin and Mitchell Catchments: A Technical Report from the CSIRO Northern Australia Water Resource Assessment to the Government of Australia*; CSIRO: Canberra, Australia, 2016; p. 159.
41. Ward, D.P.; Hamilton, S.K.; Jardine, T.D.; Pettit, N.E.; Tews, E.K.; Olley, J.M.; Bunn, S.E. Assessing the seasonal dynamics of inundation, turbidity, and aquatic vegetation in the Australian wet-dry tropics using optical remote sensing. *Ecohydrology* **2013**, *6*, 312–323. [CrossRef]
42. Kennard, M.J. *Priorities for Identification and Sustainable Management of High Conservation Value Aquatic Ecosystems in Northern Australia*; Department of Sustainability, Environment, Water, Population and Communities, Darwin: Canberra, Australia, 2011; p. 72.
43. Mitsch, W.J.; Bernal, B.; Hernandez, M.E. Ecosystem services of wetlands. *Int. J. Biodivers. Sci. Ecosyst. Serv. Manag.* **2015**, *11*, 1–4. [CrossRef]
44. Gallant, J.C.; Dowling, T.I.; Read, A.M.; Wilson, N.; Tickle, P.K.; Inskeep, C. *SRTM-Derived 1 Second Digital Elevation Models Version 1.0.*; Geoscience Australia: Canberra, Australia, 2011.

45. Karim, F.; Pena-Arancibia, J.; Ticehurst, C.; Marvanek, S.; Gallant, J.C.; Hughes, J.; Dutta, D.; Vaze, J.; Petheram, C.; Seo, L.; et al. *Floodplain Inundation Mapping and Modelling for the Fitzroy, Darwin and Mitchell Catchments: A Technical Report from the CSIRO Northern Australia Water Resource Assessment to the Government of Australia*; Commonwealth Scientific and Industrial Research Organisation: Canberra, Australia, 2018; p. 171.
46. Lymburner, L.; Tan, P.; Mueller, N.; Thackway, R.; Lewis, A.; Thankappan, M.; Randall, L.; Islam, A.; Senarath, U. *The National Dynamic Land Cover Dataset*; 2011/31; Geoscience Australia: Canberra, Australia, 2011; p. 105.
47. Chow, V.T. *Open Channel Hydraulics*; McGraw-Hill International Edition: Singapore, 1959; p. 680.
48. LWA. *An Australian Handbook of Stream Roughness Coefficients*; Land and Water Australia: Canberra, Australia, 2009; p. 28.
49. DHI. *MIKE21 Flow Model FM, Hydrodynamic Module, User Guide*; DHI Water and Environment Pty Ltd: Horsholm, Denmark, 2016.
50. Gringorten, I.I. A Plotting Rule for Extreme Probability Paper. *J. Geophys. Res.* **1963**, *68*, 813–814. [CrossRef]
51. Karim, F.; Kinsey-Henderson, A.; Wallace, J.; Arthington, A.H.; Pearson, R.G. Modelling wetland connectivity during overbank flooding in a tropical floodplain in north Queensland, Australia. *Hydrol. Processes* **2012**, *26*, 2710–2723. [CrossRef]
52. Mueller, N.; Lewis, A.; Roberts, D.; Ring, S.; Melrose, R.; Sixsmith, J.; Lymburner, L.; McIntyre, A.; Tan, P.; Curnow, S.; et al. Water observations from space: Mapping surface water from 25 years of Landsat imagery across Australia. *Remote Sens. Environ.* **2016**, *174*, 341–352. [CrossRef]
53. Godfrey, P.C.; Arthington, A.H.; Pearson, R.G.; Karim, F.; Wallace, J. Fish larvae and recruitment patterns in floodplain lagoons of the Australian Wet Tropics. *Mar. Freshwater Res.* **2017**, *68*. [CrossRef]
54. IPCC. *Climate Change 2014, Synthesis Report, Contribution of Working Groups I, II and III to the Fifth Assessment Report of the Intergovernmental Panel on Climate Change*; IPCC: Geneva, Switzerland, 2014; p. 151.
55. Hughes, J.; Yang, A.; Wang, B.; Marvanek, S.; Carlin, L.; Seo, L.; Petheram, C.; Vaze, J. *Calibration of river System and Landscape Models for the Fitzroy, Darwin and Mitchell Catchments: A Technical Report from the CSIRO Northern Australia Water Resource Assessment to the Government of Australia*; CSIRO: Canberra, Australia, 2017; p. 129.